

Supporting Information

Three-Electron Reversible Redox for High-Energy Fluorophosphate cathode- $\text{Na}_3\text{V}_2\text{O}_2(\text{PO}_4)_2\text{F}$

Manhua Peng,^a Dongtang Zhang,^a Xiayan Wang,^{*a} Dingguo Xia,^b Yugang Sun,^c and
Guangsheng Guo^a

^a *Beijing Key Laboratory for Green Catalysis and Separation, Department of Chemistry and
Chemical Engineering, Beijing University of Technology, Beijing 100124, P.R. China.*

^b *Key Lab of Theory and Technology for Advanced Batteries Materials, College of Engineering,
Peking University, Beijing 100871, P.R. China.*

^c *Department of Chemistry, Temple University, Philadelphia, Pennsylvania 19122, USA.*

* *Tel: +86 10 6739 6493; E-mail: xiayanwang@bjut.edu.cn*

Experimental

Synthetic procedures

Square piece electrode materials with good crystallinity were synthesized by reversed-phase microemulsion.^[1] The concentration of the aqueous solution was 0.2 mol/L, and the molar ratio of water and surfactant was 1:10. For synthesis of crystal clusters, polyethylene glycol 200 was used as a solvent to replace polyethylene glycol 400, and the concentration of the aqueous solution was 0.1 mol/L (crystal cluster (2)) and 0.2 mol/L (crystal cluster (1)). In addition, irregular secondary particles formed by the aggregation of primary particles were also synthesized.^[2]

Carbon-coated crystal clusters were carried out by using sucrose as a carbon precursor. The molar ratio of crystal clusters material and sucrose was 2:1, then they were dispersed in deionized water of 10 mL and stirred evenly. Afterwards, the solution was placed in an oven and dried at 120 °C. The dry materials obtained were placed in a tube furnace for 15 min at 550 °C under argon atmosphere.

[1] M. Peng, B. Li, H. Yan, D. Zhang, X. Wang, D. Xia and G. Guo, *Angew. Chem. Int. Ed.* 2015, **54**, 6452-6456.

[2] M Peng, D Zhang, L Zheng, X Wang, Y Lin, D Xia, Y Sun and G Guo. *Nano Energy* 2017, **31**,64-73.

Materials and methods

X-ray diffraction was used to characterize the phase of the composite materials via a D8ADVANCE DAVINCI instrument (Bruker, Germany), and the Cu target was used as an emission source (wavelength 1.5418 Å). An XRD diffraction pattern was refined by Material studio software 2017. Hitachi S-4300 and transmission electron microscope Tecnai G2 F20 (FEI, USA) were used to analyze the material morphology.

The electrochemical performance of the synthesized electrode material was tested. The active material, acetylene black, and binder were mixed at a molar ratio of 70:20:10 to produce the electrode sheet, and then the electrode sheet was cut into a small disc with a mass of approximately 0.3 ~ 0.5 mg and kept in an oven at 100 °C for 10 h. A total of 1 mol/L NaClO₄ (propylene carbonate as a solvent with 2% added Fluoroethylene carbonate) was used as an electrolyte. Grade GF/D glass fiber (Whatman, USA) was used as the separator. A pure sodium piece was used as the anode material, and the cells were assembled in a glove box filled with argon. The electrochemical test was performed at room temperature using a NEWARE battery testing system.

The migration barrier of the mono-vacancy migration mechanism of sodium ions was calculated by material studio software 2017. The Dmol3 package was used, and the GGA and Perdew-Wang (PW91) density function was adopted for the exchange correlation; spin polarization was totally unrestricted, and symmetry was used. A Monkhorst-Pack k-point of 1*1*2 with an orbital occupancy smearing of 0.05 Ha was used in a superlattice of 2*2*1.

The calculated parameters are already listed in the experimental section, and there are two migration paths. See Figure 4a, one migration path is in the red frame, the sodium ion migrates along the four sodium ion vacancies (black arrow), The other path is the sodium ion migration between the red frames (purple arrow). Figure 4b is a structure in which sodium ions correspond to the initial state and the final state of the two migration paths. TS is an intermediate structure.

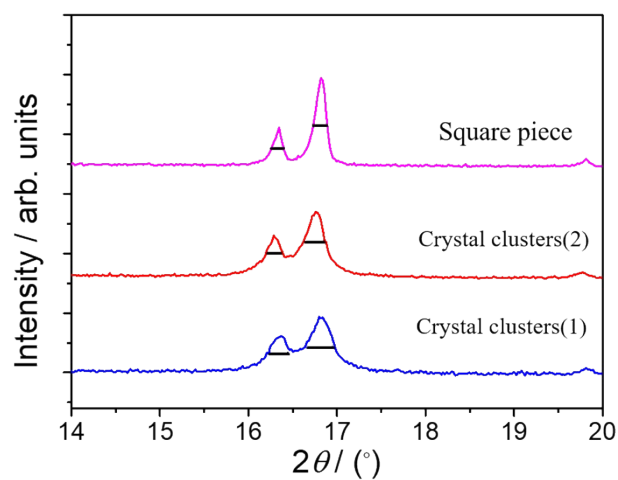


Fig.S1 14~20° XRD patterns of three materials.

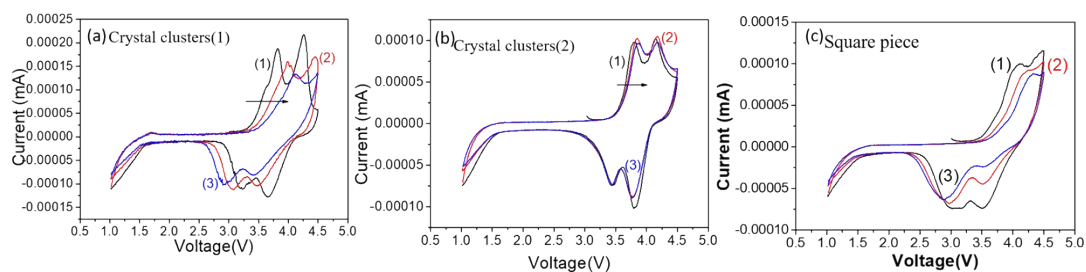


Fig.S2 Three CV curves of crystal clusters (1) (a), crystal clusters (2) (b), square piece (c). The CV curves of the three samples showed polarization state as a normal phenomenon. The polarization of samples is related with CV rate, particle size and conductivity. For example, the more obvious the polarization is, the bigger the CV rate is. As to the more serious polarization in Fig. S2c, that is because the size of square piece is the biggest among three samples.

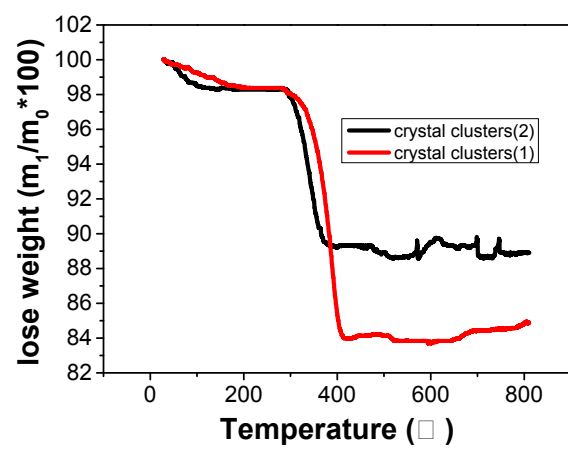


Fig.S3 TG curves of crystal clusters (1) (a), crystal clusters (2) after coated

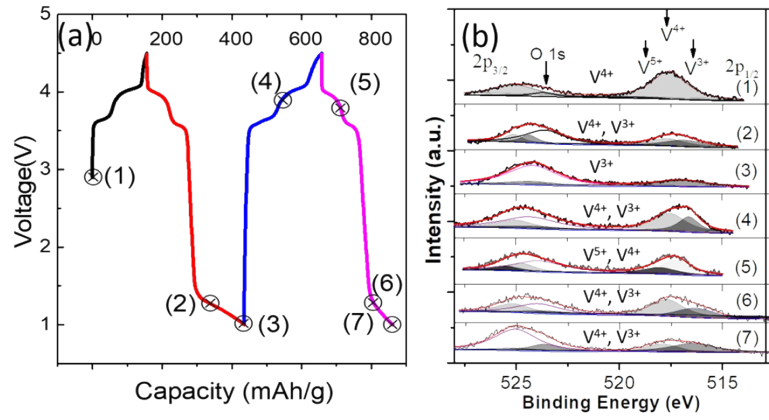
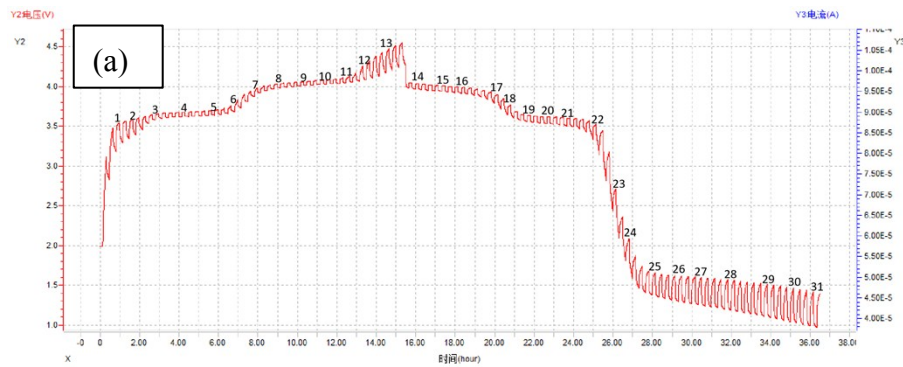


Fig.S4 (a) Different cut-off voltage; (b) X-ray Photoelectron Spectroscopy of crystal clusters obtained at different cut-off voltage of charge-discharge process (Fig.S5a).



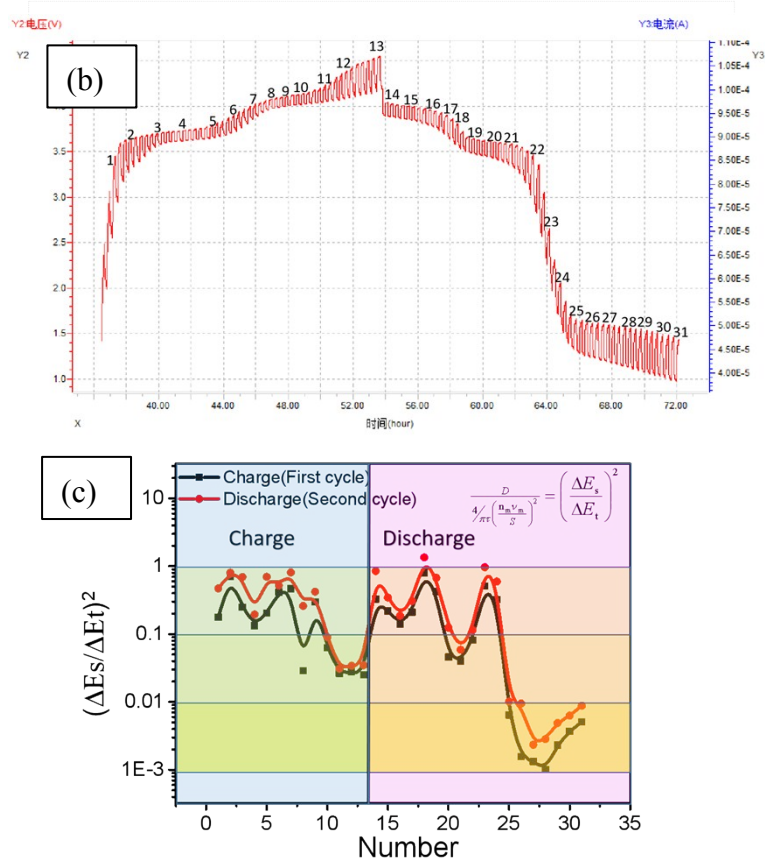


Fig.S5 GITT data at first cycle (a) and the second cycle (b);(c) $\left(\frac{\Delta Es}{\Delta Et}\right)^2$ from above

measured data, D as diffusion coefficient. number as 1~31. i is current, n_m is mole number; v_m is electrode molar volume; S is contact area of electrode and electrolyte.

$\frac{4}{\pi\tau} \left(\frac{n_m v_m}{S}\right)^2$ as a constant a . So $D = a \left(\frac{\Delta Es}{\Delta Et}\right)^2$, then you can directly compare diffusion

efficients via $\left(\frac{\Delta Es}{\Delta Et}\right)^2$, which we can easily obtained.

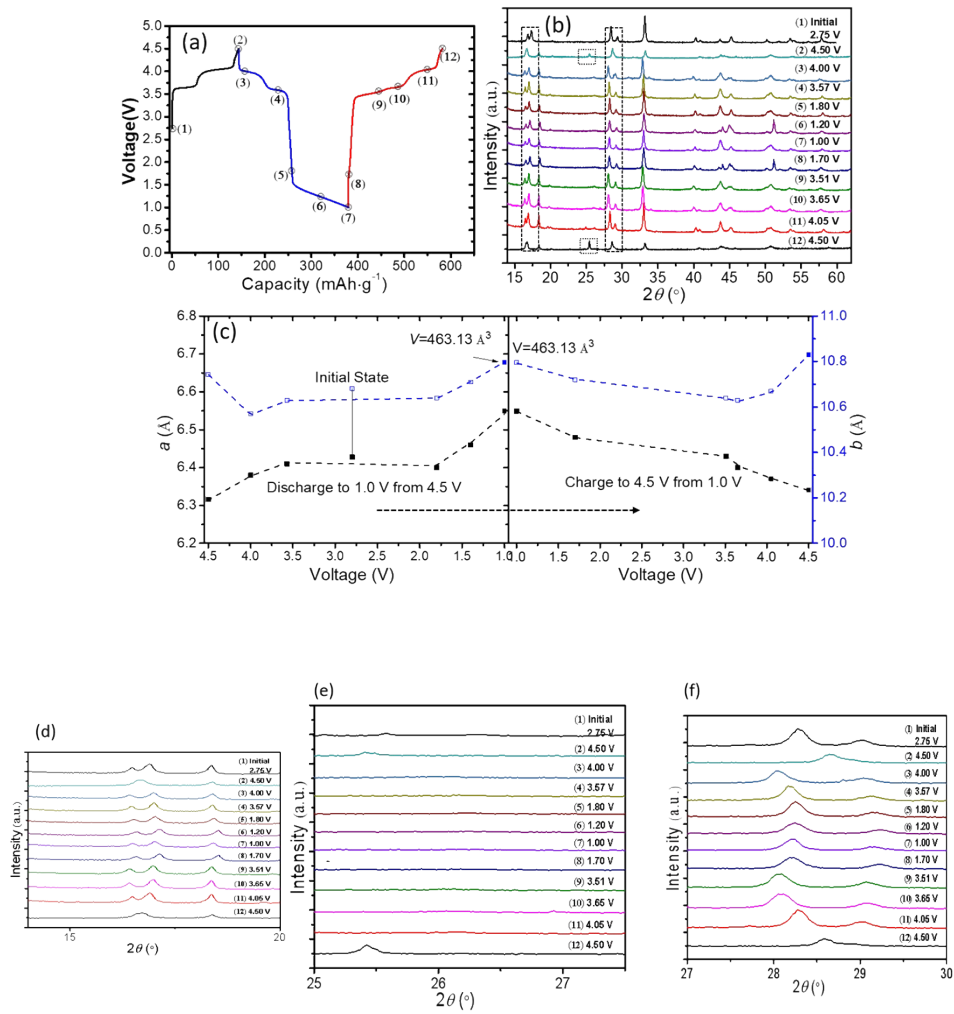


Fig.S6 Phase change analysis of the XRD pattern. (a) charge and discharge curves, (b) XRD patterns measured at different cutoff voltages, and (c) the obtained cell parameters.(d~e) amplified windows for the selected areas in Fig. S6b.